

# **CLIMATE CHANGE IMPACTS ON THE COASTAL SEA LEVEL EXTREMES OF THE EAST-CENTRAL MEDITERRANEAN SEA**

**C. Makris\*, P. Galiatsatou, Y. Androulidakis, K. Kombiadou, V. Baltikas, Y. Krestenitis and P. Prinos**

Division of Hydraulics & Environmental Engineering, Department of Civil Engineering, A.U.Th.,  
GR- 54124, Thessaloniki, Greece

\*Corresponding author: e-mail: [cmakris@civil.auth.gr](mailto:cmakris@civil.auth.gr), tel: (+30) 2310 995708

## **Abstract**

Extreme events of sea level elevation, due to severe weather conditions, pose great threats to low-land coastal areas by extended inundation hazards. The latter take the form of short- to mid-term flooding due to wave- and storm-induced sea level elevation and run-up on the coast. In this paper, the impact of the combined effect of extreme storm surges and extreme wave set-up in nearshore areas is investigated. The framework is set by future and historic climate change scenarios during a period of 150 years (1951–2100) that affect the occurrence frequency and magnitudes of total (surge- and wave-induced) sea level extremes in the eastern Mediterranean, focusing on the coastal zones of Greece. Inter-annual and multi-decadal patterns, trends and return levels of storm surge and wave set-up extremes are calculated based on non-stationary bivariate statistical analysis with copula functions of the Generalized Extreme Value distribution. The numerical data of storm surge- and wave-induced sea levels are derived from post-processing of simulation results by GreCSS and SWAN models, respectively, in order to transfer validated numerical data from offshore regions towards the shoreline of selected areas prone to coastal flooding. An increase and a consequent attenuation of storminess and inter-annual extremes of total sea level on the coast is estimated during the 1<sup>st</sup> and 2<sup>nd</sup> half of the 21<sup>st</sup> century, respectively. Different morphological characteristics of regional coastal zones in the Aegean Sea are found to influence variability of sea level extremes.

**Keywords:** Storm surge, Wave set-up, Extremes, Mediterranean Sea, Climate change impact

## **1. INTRODUCTION**

Harsh weather conditions can cause extreme events of sea level elevation (SLE) in the marine environment possibly leading to extended coastal flooding that has severe environmental and societal impacts, such as loss of land and damages to onshore infrastructure, coastal structures and ports. In the framework of a constantly changing climate with extreme SLE events of higher frequency and intensity, both augmented by the estimated mean sea level (MSL) rise, the exposure and vulnerability of society, infrastructure and the environment of coastal areas to severe damages are expected to increase. The effect of climate change on the coastal zones of the Mediterranean and other Seas around Europe has been studied in the past (Benetazzo et al., 2012; Conte and Lionello, 2013; Kvočka et al., 2016; Vousdoukas et al., 2016; Satta et al., 2017; Vibilić et al., 2017), mostly focusing on the variability and long-term trends in the evolution patterns of MSL rise, and the extremes of storm surge events and waves, yet in a separative approach for the several hydraulic features contributing in total SLE.

Our former work has been centered on proper implementation of extremal analysis for hydraulic features in the marine environment (Galiatsatou, 2007; Galiatsatou and Prinos, 2008, 2014, 2015;

Galiatsatou et al., 2016) and validated hydrodynamic modeling of storm surges and waves in coastal zones (Krestenitis et al., 2014, 2015; Androulidakis et al., 2015; Makris et al., 2015, 2016). In the aforementioned studies, the impacts of climate change on the extremes of storm surges and waves have been investigated (taking into account the MSL rise) in selected areas of the Mediterranean, Aegean and Ionian Seas, detecting a considerable increase in the extreme wave/surge climate especially in the 1<sup>st</sup> half of the 21<sup>st</sup> century. Yet, former literature has focused on analysis of SLE extremes treating storm surge and severe wave events separately. Only recently Feng et al. (2018) and Galiatsatou et al. (2017, 2018) have made efforts to study storm flood-prone coastal areas based on coupled surge-wave simulations and recent advances in extreme analysis with copula functions (Wahl et al., 2012; Bender et al., 2014), respectively. In the present work, a non-stationary multivariate approach has been developed and implemented to assess design total water levels at the shoreline of selected Greek coastal areas in the Aegean Sea under the effects of climate change.

## 2. METHODOLOGY

### 2.1 Methodological approach and topographical characteristics of the study area

The methods and techniques of the present work have been implemented to the annual maxima of random wave characteristics (*i.e.* significant wave height  $H_s$  and corresponding peak spectral period  $T_p$ ) in open seas, nearshore wave-induced sea level  $\eta_w$ , and associated SLE values due to storm surges at selected locations of the east central Mediterranean (Aegean Sea). Three representative high flood-risk study areas (Makris et al., 2016; Galiatsatou et al., 2017, 2018) have been selected (Figure 1); Area 1 in the North Aegean containing the coastal zone of Alexandroupolis and part of the Thracian Sea, Area 2 in the Central Aegean containing the coast of Eresos in southern Lesvos Island, and Area 3 in the South Aegean containing a northern Crete coastal area of Heraklion. The selection of representative group of points was based on proper statistical homogeneity measures for high quantiles of the Hosking and Wallis type (Makris et al. 2016; Galiatsatou et al., 2017, 2018) assessed for annual maxima of  $H_s$  and SLE for a control period (1951-2000), related to its counterpart 50-year future periods in 2001-2100. High-wave events exceeding appropriately defined thresholds of  $H_s$  (1.5-2 m) were selected at grid points in the study area, for durations >6 hrs, having onshore main wave directions towards respective shorelines.  $T_p$  values were associated to the high sea states corresponding to a period of 150 years (1951-2100). The choice of SLE data was based on a 5-day time-window of storm surge-driven sea levels, covering the time of corresponding records of  $H_s$  maxima (by 2.5 days bilaterally), indicated in order to estimate the largest possible SLE response to the particular storm events (with maximum duration of 120 hrs in the Mediterranean basin; Conte and Lionello, 2013; Makris et al., 2016).

### 2.2 Numerical models and data for storm surges and waves

The raw data of marine parameters in the present work are drawn from climatic-type numerical simulations to estimate the (offshore) irregular wave characteristics ( $H_s$ ,  $T_p$  and energy wave spectrum features) from SWAN model implementations (Kapelonis et al., 2015; Makris et al., 2016), and SLE due to storm surges from 2-DH high-resolution simulations with MeCSS and GreCSS hydrodynamic models (Krestenitis et al. 2014; Androulidakis et al. 2015; Makris et al. 2015, 2016). The modelled datasets were validated and bias-corrected by *in situ* measurements, satellite altimetry and modeled forecasts, and covered a 150-year period (1951-2100), using atmospheric forcing of climatic data, produced by a dynamically downscaled simulation with RegCM3 model (Tolika et al., 2015; Vagenas et al., 2017), under 20C3M historical and SRES-A1B future scenarios for green-house gas emissions (Makris et al., 2016; Vagenas et al., 2017).

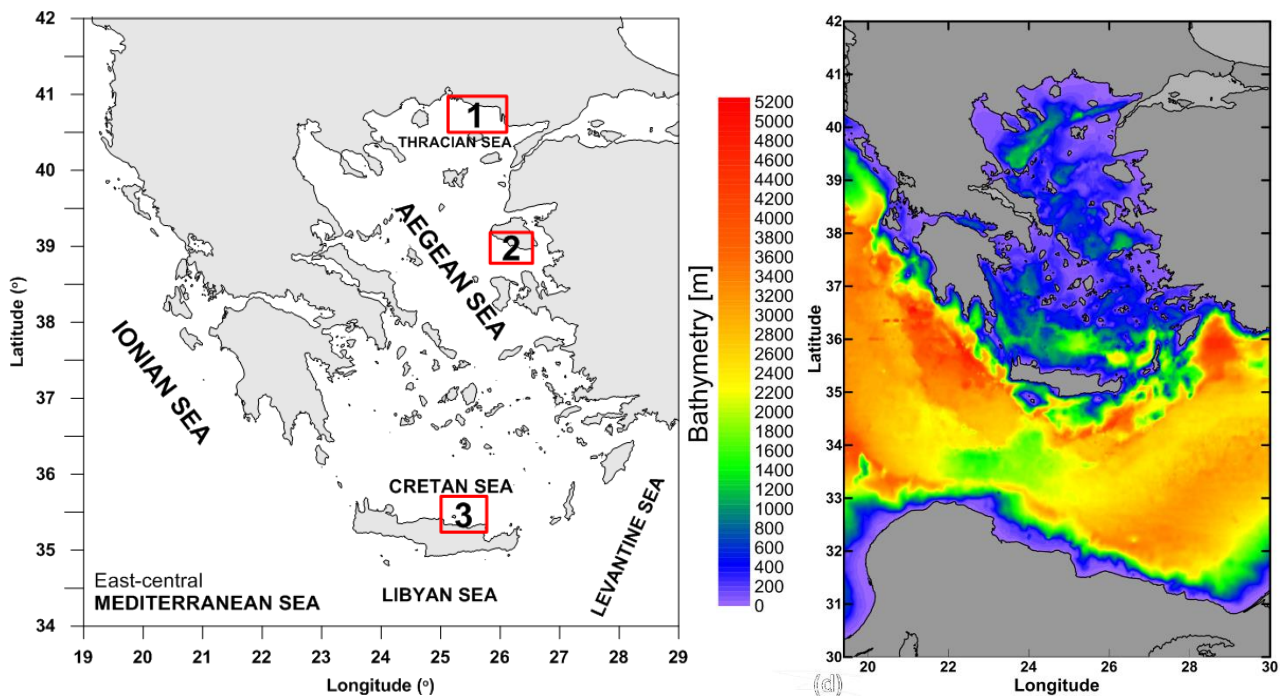


**Figure 1: Left graph: Selected study areas of the Aegean Sea; 1: Alexandroupolis coastal area in the Thracian Sea (North Aegean), 2: Eresos coastal area in southern Lesvos Island (Central Aegean), 3: Heraklion coastal area in the Cretan Sea (South Aegean). Right graph: Marine map of the study area's bathymetry (m) for the  $1/20^\circ$  (~5 Km) resolution computational domain**

### 2.3 Modelling approach for total sea level on the coast

The calculation method of the coastal hazard under investigation, *i.e.* the total (flood) water level at the shoreline and on the coast, is concisely presented in the following (detailed entire approach by Galiatsatou et al., 2018), by implementing a semi-analytic modelling approach for the derivation of the nearshore (surf/swash zone) wave-induced sea levels (Goda, 2000). In order to correctly calculate the total sea level in coastal areas, and specifically inside the surf zone and at the shoreline, we need to transfer the spatially large-scale modelled (wave and storm surge) data from relatively deep (or intermediate) waters in the open sea to nearshore shallow water areas and finally the shoreline boundary. The storm surge is a huge-scale phenomenon (order of several Km) and coastal SLE values were therefore adequately provided by dynamically downscaled numerical simulations in climatic mode (150 years,  $1/20^\circ$  resolution; Makris et al., 2015, 2016). Nevertheless, the wave-induced sea level in nearshore areas and close to the shoreline concerns finer scale effects due to irregular wave breaking. Nonetheless, numerical simulations in climatic mode (150 years) with a 2-DH wave model of very fine spatial resolution is still very arduous in terms of computational resources and available detail in digital bathymetric and terrain models. Therefore, in the present work, we used the offshore SWAN model results of Makris et al. (2016). Consequently we calculated the transformation of extreme random wave characteristics ( $H_s$ ,  $T_p$ , main wave direction) towards the shoreline with a semi-analytical iterative model for irregular wave trains (Makris and Krestenitis, 2009), which takes into account the crude variations of rather simple bathymetries (parallel depth-contours, nearly straight coastlines and uniform slopes) crossing areas of nearshore intermediate to shallow waters and surf zone  $H_s$  constraints for irregular wave breaking. Furthermore the wave-induced set-up  $\eta_{su}$  was calculated (Goda 2000), as it represents the short- to mid-term SLE in the coastal zone, due to random wave action in shallow waters and secondary processes due to irregular wave breaking. We also added another smaller component of SLE, *i.e.* the surf beat  $\eta_{sb}$ , associated to wave groups approaching coastal zones in discrete high- and low-frequency bands. Conclusively, we estimated the (potential) total wave-induced sea level  $\eta_w = \eta_{su} + \eta_{sb}$  nearshore and on the shoreline, being qualitatively similar to storm surge SLE, rendering it a fitting counterpart in a bivariate analysis of sea level values.

Transformation of random wave characteristics from open seas to shallow coastal waters was based on spectral wave theory and analytic relations of Goda (2000) taking into account irregular wave propagation, refraction, shoaling, and energy dissipation due to breaking and bottom friction. The significant wave height  $H_s$  in arbitrary depth  $d$  is given by the relation  $H_s = k_r' \cdot k_s' \cdot H_{s,o}$  (where  $o$  index corresponds to deep-water offshore values). For areas with rather parallel depth-contours, the effective spectral refraction and shoaling coefficients,  $k_r'$  and  $k_s'$ , for irregular waves are given by:

$$k_r' = f(k_r, h/L_{o,p}, a_{p,o}, s_{max}), \text{ from graphs} \quad k_r' = \sqrt{\sum_{i=1}^M \sum_{j=1}^N (\Delta E)_{ij} (k_r)_{ij}^2}, \text{ analytically} \quad (1)$$

$$k_s' = k_s, \quad d_{30} \leq d \quad k_s' = (k_s)_{30} \cdot \left(\frac{d_{30}}{d}\right)^{2/7}, \quad d_{50} < d < d_{30} \quad k_s' \cdot (\sqrt{k_s'} - B) - \Gamma = 0, \quad d < d_{50} \quad (2)$$

where  $k_r(f, \theta)$  is the linear refraction coefficient of monochromatic wave components with frequency  $f$  and propagation direction  $\theta$ ,  $(\Delta E)_{ij}$  are the components of relative wave energy with  $i$ th discrete frequency and  $j$ th angle of incidence for discrete spectral bands,  $L_{o,p}$  is the deep water wavelength corresponding to  $T_p$ ,  $H_{s,b}$  (depth-limited breaker height) and the rest parameters are (Goda, 2000):

$$\left(\frac{d_{30}}{L_{o,p}}\right)^2 = \frac{2\pi}{30} \frac{H'_{s,o}}{L_{o,p}} (k_s)_{30}, \quad \left(\frac{d_{50}}{L_{o,p}}\right)^2 = \frac{2\pi}{50} \frac{H'_{s,o}}{L_{o,p}} (k_s)_{50}, \quad B = \frac{2\sqrt{3}}{\sqrt{2\pi H'_{s,o}/L_{o,p}}} \frac{d}{L_{o,p}}, \quad \Gamma = \frac{C_{50}}{\sqrt{2\pi H'_{s,o}/L_{o,p}}} \left(\frac{L_{o,p}}{d}\right)^{3/2} \quad (3)$$

$$C_{50} = (k_s)_{50} \left(\frac{d_{50}}{L_{o,p}}\right)^{3/2} \left[ \sqrt{(k_s)_{50} \cdot 2\pi H'_{s,o}/L_{o,p}} - 2\sqrt{3} \frac{d_{50}}{L_{o,p}} \right], \quad H_{s,b} = A \cdot L_{o,p} \cdot \left\{ 1 - \exp \left[ -1.5 \cdot \frac{\pi \cdot d_{s,b}}{L_{o,p}} (1 + 15 \cdot m^{4/3}) \right] \right\}$$

where  $A=0.12-0.18$  is a shape parameter depending on the position of the broken wave inside the surf zone,  $d_{s,b}$  the incipient breaking depth of  $H_{s,b}$ , and  $m$  the bottom slope. Combining iteratively the breaking model with the random wave transformation, we calculated an estimation of the wave set-up evolution in the surf zone transverse to the coast,  $d\eta/dx$  ( $\eta_{su}$ ,  $\eta_{sb}$  exactly on the shoreline):

$$\frac{d\eta}{dx} = -\frac{1}{(\eta + d)} \cdot \frac{d}{dx} \left[ \frac{1}{8} H_s^{-2} \left( \frac{1}{2} + \frac{4\pi d/L_p}{\sinh(4\pi d/L_p)} \right) \right], \quad \eta_{su} = \frac{3\gamma^2/8}{1+3\gamma^2/8} \cdot d_b - \frac{\gamma^2 \cdot d_b}{16}, \quad \eta_{sb} = \frac{0.01 \cdot H'_{s,o}}{\sqrt{\frac{H'_{s,o}}{L_{o,p}} \left( 1 + \frac{d_{s,b}}{H'_{s,o}} \right)}} \quad (4)$$

where  $\gamma = H_{s,b}/d_{s,b}$  is the wave breaking index,  $L_p$  the local wavelength corresponding to  $T_p$ , and  $\eta$  the local value of the sea level (mean water level) due to the random breaking-induced process of the wave set-up in depth  $d$ . The estimation of the total (flood) water level at the shoreline  $\eta_t$  resulted from the summation of all the SLE components: wave run-up  $R_{2\%}$  (contains the parameter  $\eta_{su}$ ), MSL rise  $MSLR$  (due to ice melting, steric and mass addition components; Makris et al., 2016) the surf beat  $\eta_{sb}$ , the storm surge-induced SLE, and the highest astronomical tide  $HAT$  (courtesy of Hellenic Navy Hydrographic Service, <https://www.hnhs.gr/en/>):

$$\eta_t = R_{2\%} + MSLR + \eta_{sb} + SLH + HAT \quad (5)$$

where the wave run-up at the shoreline was based on the formulation of Stockdon et al. (2006):

$$R_{2\%} = 1.1 \left( 0.35 \tan \beta (H_s L_o)^{\frac{1}{2}} + \frac{(H_s L_o (0.563 \tan^2 \beta + 0.004))^{\frac{1}{2}}}{2} \right) \quad \text{and} \quad R_{2\%} = 0.043 (H_s L_o)^{\frac{1}{2}}, \quad \text{for } Ir < 0.3 \quad (6)$$

with  $\tan\beta$  the beach face slope and  $Ir=m/\sqrt{(H_{s,o}/L_{o,p})}$  the Iribarren number (surf similarity parameter). For dissipative beaches ( $Ir<0.3$ ) the wave run-up is infragravity dominated.

### 2.4 Method for extreme value analysis

Extreme value analysis in the present paper is based on the Generalized Extreme Value (GEV) distribution function, which includes location  $\mu$ , scale  $\sigma>0$ , and shape  $\xi\neq 0$  parameters, assessed by Maximum Likelihood Estimation (MLE) or L-moments (LM) procedures (computed from linear combinations of probability weighted moments), providing measures for shape of distributions or data samples, such as location, dispersion, skewness and kurtosis. For data samples of  $\{X_1, X_2, \dots, X_n\}$  arranged in increasing order, the sample probability weighted moments are:

$$b_0 = \frac{1}{n} \sum_{j=1}^n X_j, \quad b_r = \frac{1}{n} \sum_{j=r+1}^n \frac{(j-1)(j-2)\dots(j-r)}{(n-1)(n-2)\dots(n-r)} X_j \tag{7}$$

Extreme SLE values (e.g. 50-year return levels) exhibit non-stationarity, led by natural climatic variability and climate change, viz. the El Niño Southern Oscillation (ENSO) or North Atlantic Oscillation (NAO) acting on different time scales. These can have significant impacts on SLE extremes and occurrence frequency of coastal flooding events, thus assuming time-varying  $\mu, \sigma, \xi$ :

$$G(x) = \exp \left[ - \left\{ 1 + \xi(t) \frac{(x - \mu(t))}{\sigma(t)} \right\}^{-1/\xi(t)} \right], \quad 1 + \xi(t) \frac{(x - \mu(t))}{\sigma(t)} > 0 \tag{8}$$

The return level  $x_p$  corresponding to a return period  $T=1/p$  is assessed in a non-stationary context as a function of time, representing quantiles of the distribution function of SLE for every year:

$$x_p(t) = \mu(t) - \frac{\sigma(t)}{\xi(t)} \left[ 1 - \{-\log(1-p)\}^{-\xi(t)} \right] \tag{9}$$

For the estimation of the parameters of the fitted distribution functions for all sea level variables, a moving time-window of 40-years (Bender et al., 2014) was implemented in the present work, using the LM method for each period. Their length was selected to be large enough to provide a good fit of the marginal distributions of  $H_s$ , SLE, etc., as well as of their possible dependence structure. In a multivariate framework (Galiatsatou et al., 2018), the non-stationary marginal distribution functions for wave and storm surge variables has to be followed by a non-stationary joint probability analysis of the dependent variables using bivariate copulas, which model dependence structure of e.g.  $H_s$  and SLE, independently from their marginal distributions. To estimate the dependence structure of nearshore sea level data within the non-stationarity framework, 40-year moving windows were also applied to the bivariate data ( $H_s/T_p$  and  $H_s/SLE$ ), utilizing Canonical Maximum Likelihood (CML) without first specifying marginal distributions. This way, marginals are first transformed to pseudo-observations with uniform margins  $(U_{i1}, U_{i2})^T$  and then the dependence parameter  $a$  is estimated as:

$$\hat{a}_{CML} = \operatorname{argmax}_a \sum_{i=1}^n \log c(U_{i1}, U_{i2}; a) \tag{10}$$

To select the appropriate copula function among five candidates (i.e. Clayton, Frank, Gumbel, Student’s t, Gaussian), a parametric bootstrap procedure has been used (Galiatsatou et al., 2017, 2018). The test computes the Cramér – von Mises functional  $S_n$ , comparing the empirical copula of the observations with a parametric estimate of the copula derived under the null hypothesis. Approximate  $p$ -values for the test have been computed using the parametric bootstrap procedure. Large values of  $S_n$  usually result in the rejection of the null hypothesis that the bivariate data result from the tested copula function. After estimating the copula parameters, the statistic  $S_n$  and its associated  $p$ -value were estimated for all moving windows and all candidate copula functions. For

each bivariate pair, the copula that resulted in  $p$ -values exceeding the 5% significance level for the entire study period, was selected as the best-fit model and applied for joint exceedance probability estimation. In case more than one of the fitted copulas satisfied the above condition, the selected bivariate model was the one providing the lowest Akaike Information Criterion (AIC) values during the largest part of the studied time interval (Galiatsatou et al., 2017, 2018).

### 3. RESULTS

#### 3.1 Numerically simulated data

Results for the 50-year patterns of  $H_s$  annual maxima in the study area are presented in Figure 2. A projected increase of the Etesian winds at the central part of the Aegean (Tolika et al., 2015; Makris et al., 2016) seems to be responsible for a small but traceable change in  $H_{s,max}$  patterns during 2001-2050. Intensification trends are mainly estimated to occur in the northern and central parts of the Aegean Sea, with smaller values in the southern parts of the study area. An increase of  $H_{s,max}$  in the Ionian and Libyan Seas during the 1<sup>st</sup> half of the 21<sup>st</sup> century and a consequent attenuation towards 2100, follows the climate change patterns of mean sea states (not shown here). During the low-energy seasons, the entire study area reveals a consistent invariance. Figure 3 presents the spatial variability of the averaged (for each of the three periods) values of the Storm Surge Index (SSI), which is a representative annual maximum SLE, *i.e.* yearly mean of three maxima storm surge events (Androulidakis et al., 2015; Makris et al., 2016), over each 50-year period ( $SSI_{50-yr}$ ). The highest SSI values ( $>0.45$  m) can be traced along the northern coasts of the Aegean Sea (coastal zone of Alexandroupolis; Area 1). The SSI decreases from North to South, ranging from 0.32 to 0.38 m for central parts of the Aegean, down to almost 0.3 m in the southern part of the study area (Crete), and below 0.25 m for the northern African coasts. Lower values occur along the entire coastline in the 2<sup>nd</sup> half of the 21<sup>st</sup> century, consistent with the estimated storm attenuation towards 2100. The change signals between 2001-2050 and 1951-2000 range from  $-5.1$  to  $+19.6$  % locally. Storm surge-induced SLE is estimated to generally decrease from the current to the future 50-year period, with changes of  $-17.5$  to  $+1.8$  %.

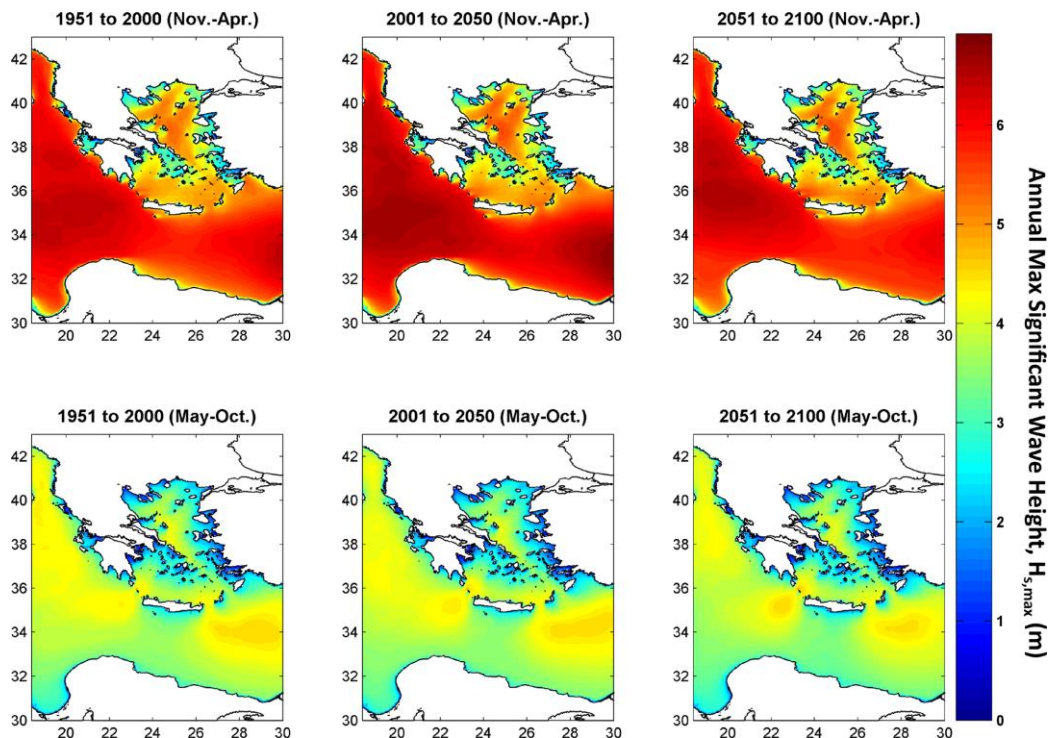


**Figure 2: Temporal mean of  $H_s$  annual maxima (m) during high- and low-energy (upper and lower graphs, respectively) months over the study area for 50-year reference (left graphs), current (central graphs) and future (right graphs) period time intervals**

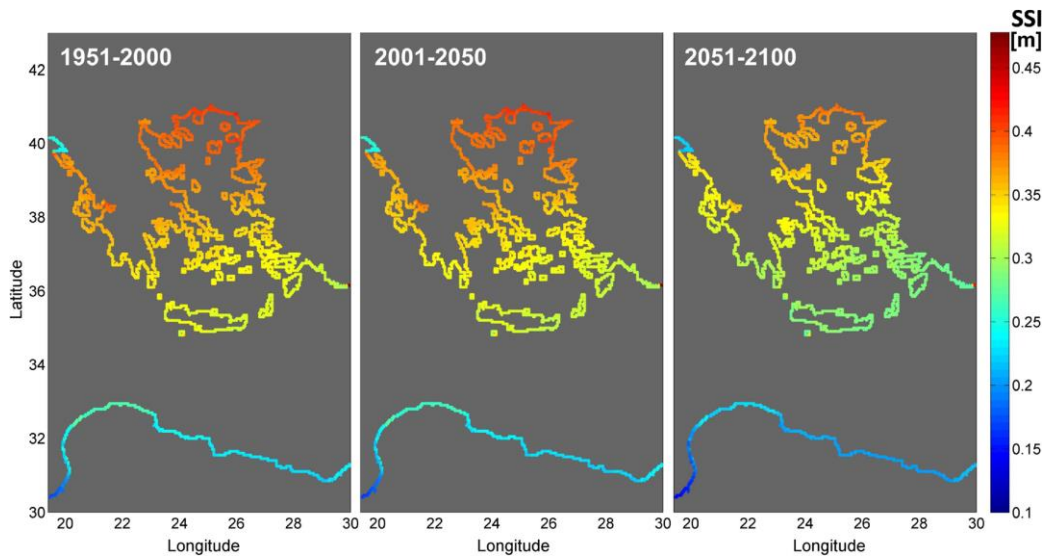


**Figure 3: Storm Surge Index SSI (m) along the coastline of the study area, time-averaged over 50-year reference, current and future periods (from left to right)**

### 3.1 Extremes and return values of storm surges, waves, and total sea level on the coast

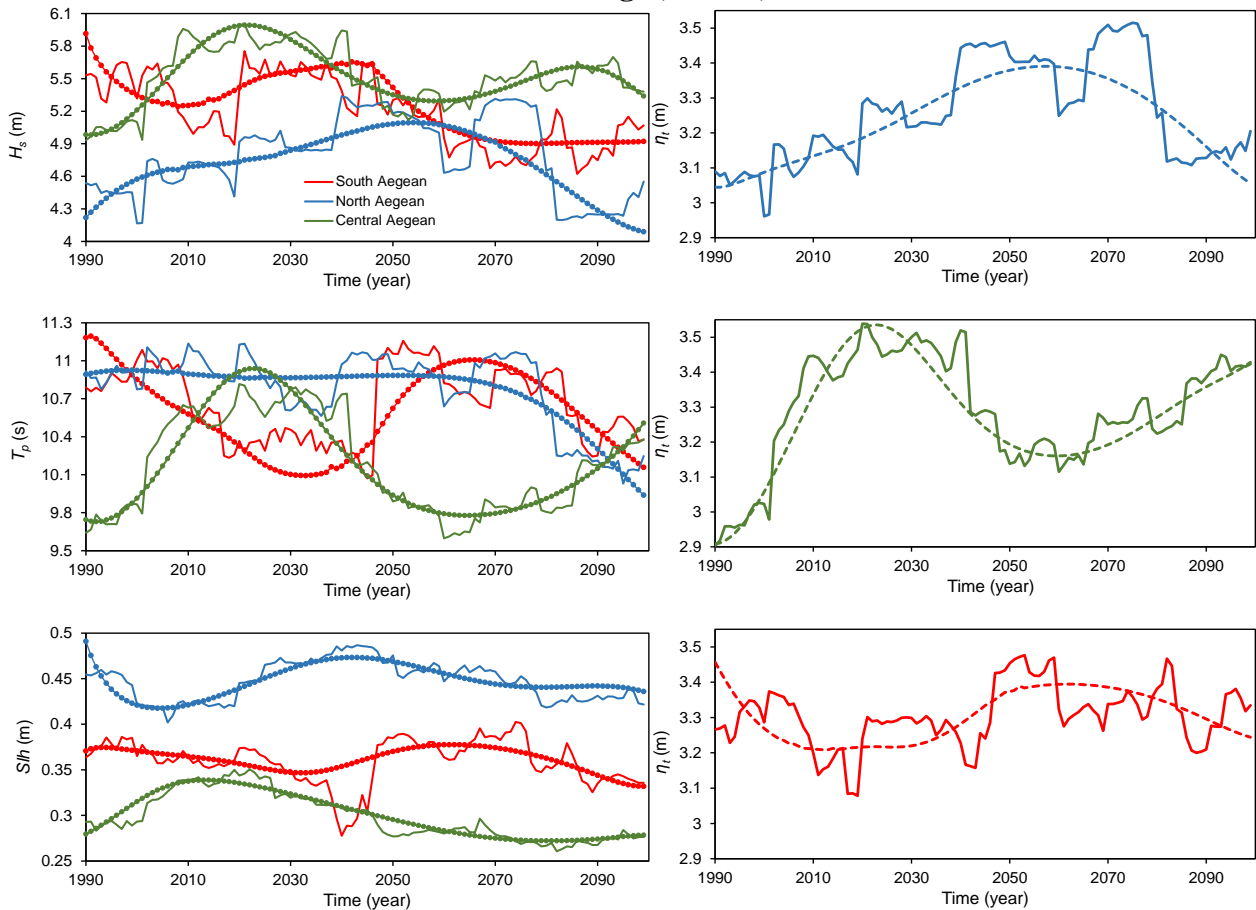


**Figure 4: Left panel: Time-dependent estimates of MLE wave event of  $H_s$  (top graph),  $T_p$  (middle graph) and SLE (lower graph) in North Aegean (blue plots), central Aegean (green plots), and South Aegean (red plots). Right panel: Time-dependent estimates of total water level at the shoreline  $\eta_t$  at selected profiles in the coastal areas of Alexandroupolis (top), Eresos bay (middle) and Heraklion (bottom). Solid lines represent MLE extracted without parametric trends in marginals and dependence parameter of bivariate data; Dot-lines consider all fitted trends**

Figure 4 (left panel graphs) presents the time-dependent most likely design estimates of  $H_s$ ,  $T_p$  and SLE for the three studied areas in the Aegean Sea. In the North Aegean Sea,  $H_s$  MLE maxima appeared in the 2<sup>nd</sup> half of the 21<sup>st</sup> century, around 2060, when including the parametric trends in the marginal parameters and the dependence structure of the marine variables. Excluding parametric trends, MLE  $H_s$  showed a bimodal behavior with pronounced peaks for short periods before and after 2050. MLEs of  $T_p$  (thus wave lengths too) are estimated to decrease rapidly during the last 30 years of the 21<sup>st</sup> century. MLE of storm surge SLE presented more than 16% variations with maxima probably occurring before the middle of the 21<sup>st</sup> century. In the Central Aegean Sea, MLEs of wave features presented more intense variability (e.g. two distinct peaks for  $H_s$ , pronounced around 2020 and towards 2085, with  $T_p$  peaking around 2020, too). A progressive decrease of MLEs for storm-induced SLE is obvious after a peak in 2010-2015. In the South Aegean Sea, the most likely design events of  $H_s$ ,  $T_p$  and SLE presented almost 22%, 10% and 37% variations, respectively. Wave heights are estimated to decrease in the 2<sup>nd</sup> half of the 21<sup>st</sup> century, while wave periods are expected to increase quite sharply in 2031-2070 and decrease rapidly during 2071-2100. SLE variation followed the  $T_p$  trend peaking around 2060.

Figure 4 (right panel graphs) presents  $\eta_t$  in the 1990-2100 interval for three selected coastal profiles having quite similar beach face slopes (7-8%) in each study area. Beach breadths varied from 14 to 40 m with berm heights from 2 to 3.2 m. In Alexandroupolis (Area 1)  $\eta_t$  varied more than 17% in the 21<sup>st</sup> century with highest values probably occurring in the 2<sup>nd</sup> half of the 21<sup>st</sup> century (*i.e.* around 2060 with parametric trends in marginal distributions and dependence structure of marine variables). The variations of total water extremes presented similar trends to those of  $H_s$  MLEs. In Eresos (Area 2),  $\eta_t$  variations exceeded 20% in 1990-2100 with maxima of total water level at the shoreline appearing after 2020, presenting similar trends to all marine variables in the area, with wave parameters (especially  $T_p$ ) having a stronger influence on them. Finally, in the coastal area of Heraklion (Area 3)  $\eta_t$  varies more than 12% in the 21<sup>st</sup> century, with its maxima around 2060 (or just after 2080 for no parametric trends in marginals and dependence parameter of bivariate data). Total water levels on the coast seem to most likely increase after 2030 maintain quite high values in the 2<sup>nd</sup> half of the 21<sup>st</sup> century. Wave periods and storm surges are estimated to heavily influence  $\eta_t$  while high waves appeared less correlated with it compared to central and northern Aegean areas.

#### 4. DISCUSSION AND CONCLUSIONS

In the present study, a novel approach has been developed and applied to selected Greek coastal areas of the Aegean Sea to investigate the changes in the joint probabilities of extreme marine variables (storm surge- and wave-induced sea level elevations) with time. The scope was to properly assess design magnitudes of total (flood) water levels at the shoreline of extended, rather homogenous, coastal areas, under the effect of climate change (based on a rather pessimistic future scenario). The results of coupled, large-scale, numerical simulations of 2-DH hydrodynamic circulation for storm surges and 3<sup>rd</sup> generation spectral wave transformation, are post-processed and blended with an irregular wave transformation model for wave-induced sea level in nearshore areas and towards the shoreline, leading to a novel, robust, analytic approach for extreme run-up and total flood water levels on the coast (Galiatsatou et al., 2018), modeling dependence structure with the use of copulas. The non-stationary analysis of the marginal distributions of all marine variables revealed statistically significant trends in all parameters of the GEV at the selected areas of the Aegean Sea. Statistically significant polynomial trends were also detected in the dependence structure of both offshore and nearshore bivariate data. Variations in future trends for probable coastal flooding might be attributed to geographical differentiations correlated to climate change signals of weather data (Makris et al., 2016) and variations of marine variable (storm wave and surge characteristics) extremes (Galiatsatou et al., 2017) in the area. The highest values of total water levels on the shoreline were calculated either around 2020 or the middle of the 21<sup>st</sup> century, while the regime of long wave sea states was correlated (significant influence) on extreme  $\eta_t$  estimates. The spatial differentiations of the patterns of extreme marine variables, based on the intense topographical diversity of the Aegean archipelago, revealed



different results of former studies (Galiatsatou and Prinos, 2014, 2015; Makris et al., 2016), implying the rise of extreme southerly winds in the Aegean Sea towards the middle of the 21<sup>st</sup> century and beyond (corroborated by Vagenas et al., 2017). In the South Aegean, the Aeolian patterns show a mild rise of northerly extreme winds after the 1<sup>st</sup> half of the 21<sup>st</sup> century, which might lead to an increase of extreme peak periods and respective storm surges that are slightly intensified. Nevertheless, due to the complex dense insular formation of the Cyclades, the random wave fields are prone to diffraction, and this seems to cause a slight drop in the significant wave height extremes. These findings (a 20- to 30-year transition of extreme sea level response to climate change on the coastal zone) are different from former studies (Galiatsatou and Prinos, 2014, 2015; Makris et al., 2016), which have shown clear patterns of storminess augmentation in the 1<sup>st</sup> half, and consequent severe attenuation in the 2<sup>nd</sup> half of the 21<sup>st</sup> century. In the Central Aegean, a more coherent pattern of sea level response to climate change signals can be traced, with the shift in the patterns of extreme values of coastal marine parameters following climatic-type changes in northerly and southerly extreme winds, giving rise in sea level extremes around 2020, which is in agreement with relevant previous literature (involving analyses with A1B scenario). Therefore, the proposed novel approach of extreme value calculation (incl. non-stationarity, time-dependence, bivariate analysis of extremes, transferring sea-states from offshore to coastal areas) can produce significant alterations on the patterns of extreme total sea levels on the shoreline, compared to former studies of univariate stationary approaches, providing somewhat safer estimates and thus more reliable risk assessment tools for coastal flooding under the effects of climate change.

## References

1. Androulidakis, Y.S. et al. (2015). 'Storm surges in the Mediterranean Sea: Variability and trends under future climatic conditions'. **Dynamics of Atmospheres and Oceans**, 71, pp. 56-82.
2. Bender, J., Wahl, T. and Jensen, J. (2014). 'Multivariate design in the presence of non-stationarity'. **Journal of Hydrology**, 514, pp. 123-130.
3. Benetazzo, A. et al. (2012). 'Wave climate of the Adriatic Sea: a future scenario simulation'. **Natural Hazards and Earth System Sciences**, 12(6), pp. 2065-2076.
4. Conte, D. and Lionello, P. (2013). 'Characteristics of large positive and negative surges in the Mediterranean Sea and their attenuation in future climate scenarios'. **Global and Planetary Change**, 111, pp. 159-173.
5. Feng, X. et al. (2018). 'Study of storm surge trends in typhoon-prone coastal areas based on observations and surge-wave coupled simulations'. **International Journal of Applied Earth Observation and Geoinformation**.
6. Galiatsatou, P. (2007). 'Joint exceedance probabilities of extreme waves and storm surges'. **XXXIII IAHR Congress**, pp. 780.
7. Galiatsatou, P. and Prinos, P. (2008). 'Non-stationary point process models for extreme storm surges'. **Flood Risk Management: Research and Practice: Proc. Floodrisk 2008**, Oxford, 1045-1054.
8. Galiatsatou, P. and Prinos, P. (2014). 'Analysing the effects of climate change on wave height extremes in the Greek Seas'. **ICHE 2014**, Hamburg, Lehfeldt & Kopmann (eds), pp. 773-781.
9. Galiatsatou, P. and Prinos, P. (2015). 'Estimating the effects of climate change on storm surge extremes in the Greek Seas'. **36<sup>th</sup> IAHR World Congress**, The Hague, The Netherlands.
10. Galiatsatou, P., Anagnostopoulou, C. and Prinos, P. (2016). 'Modelling nonstationary extreme wave heights in present and future climates of Greek Seas'. **Water Science and Engineering**, 9(1), pp. 21-32.

11. Galiatsatou, P., Makris, C. and Prinos, P. (2017). 'Non-Stationary Joint Probability Analysis of Extreme Marine Variables to Assess Design Water Levels at the Shoreline in a Changing Climate'. **3<sup>rd</sup> International EVAN Conference**, 5-7 September 2017, Southampton, UK.
12. Galiatsatou, P. et al. (2018). 'Nonstationary joint probability analysis of extreme marine variables to assess design water levels at the shoreline in a changing climate'. **Natural Hazards**, Springer. (*submitted, under review*).
13. Goda Y. (2000). '**Random Sea and Design of Maritime Structures**'. World Scientific.
14. Kapelonis, Z.G., Gavriliadis, P.N. and Athanassoulis, G.A. (2015). 'Extreme value analysis of dynamical wave climate projections in the Mediterranean Sea'. **Procedia Computer Science**, 66, pp. 210-219.
15. Krestenitis, Y. et al. (2014). 'Modeling storm surges in the Mediterranean Sea under the A1B climate scenario'. **12<sup>th</sup> COMECAP**, Heraklion (Crete), Greece, 28-31 May 2014, pp. 91-95.
16. Krestenitis, Y. et al. (2015). 'Evolution of storm surge extreme events in Greek Seas under climate change scenario'. **11<sup>th</sup> Pan-Hellenic Symposium on Oceanography and Fisheries**, Mytilene, Lesvos, Greece, 13-17 May 2015, pp. 849-852.
17. Kvočka, D., Falconer, R.A. and Bray, M. (2016). 'Flood hazard assessment for extreme flood events'. **Natural Hazards**, 84(3), pp. 1569–1599.
18. Makris, C.V. et al. (2015). 'Numerical Modelling of Storm Surges in the Mediterranean Sea under Climate Change'. **36<sup>th</sup> IAHR World Congress**, The Hague, The Netherlands.
19. Makris, C. et al. (2016). 'Climate change effects on the marine characteristics of the Aegean and Ionian Seas'. **Ocean Dynamics**, 66(12), pp. 1603-1635.
20. Makris, C.V. and Krestenitis, Y.N. (2009). 'Free Educational Software on Maritime Hydrodynamics, Coastal Engineering and Oceanography'. **9<sup>th</sup> Pan-Hellenic Symposium of Oceanography and Fisheries**, Vol.1, pp. 546-551. (*in Greek*)
21. Satta, A. et al. (2017). 'Assessment of coastal risks to climate change related impacts at the regional scale: The case of the Mediterranean region'. **International Journal of Disaster Risk Reduction**, 24, pp. 284-296.
22. Stockdon, H.F. et al. (2006). 'Empirical parameterization of setup, swash, and runup'. **Coastal Engineering**, 53, pp. 573-588.
23. Tolika, K. et al. (2015). 'A comparison of the updated very high resolution model RegCM3\_10km with the previous version RegCM3\_25km over the complex terrain of Greece: present and future projections'. **Theoretic and Applied Climatology**, pp. 1–12.
24. Wahl, T., Mudersbach, C. and Jensen, J. (2012). 'Assessing the hydrodynamic boundary conditions for risk analyses in coastal areas: a multivariate statistical approach based on copula functions'. **Natural Hazards and Earth System Sciences**, 12, pp. 495-510.
25. Vagenas, C., Anagnostopoulou, C. and Tolika, K. (2017). 'Climatic Study of the Marine Surface Wind Field over the Greek Seas with the Use of a High Resolution RCM Focusing on Extreme Winds'. **Climate**, 5(2), pp. 29.
26. Vilibić, I. et al. (2017). 'The Adriatic Sea: A long-Standing Laboratory for Sea Level Studies'. **Pure and Applied Geophysics**, Sea Level 2017, pp. 1-47.
27. Vousdoukas, M.I. et al. (2016). 'Projections of extreme storm surge levels along Europe'. **Climate Dynamics**, 47(9), pp. 3171-3190.